Acid resistance of goethite in nickel laterite ore from Western Australia. Part II. Effect of liberating cementations on acid leaching performance

Xiaodong Wang [a],*, Robbie G. McDonald [b], Robert D. Hart [a], Jian Li [b], Arie van Riessen [a]

[a] Centre for Materials Research, Curtin University, Bentley, WA 6102, Australia
[b] Division of Process Science and Engineering, CSIRO, PO Box 7229, Karawara, WA 6152, Australia

ARTICLE INFO

ABSTRACT

The acid resistance of some West Australian laterite ores has been reported to be associated with its cementation structure at submicron level. Although closely related, iron and silicon are found not to be intimately mixed in the goethite-silica/silicate cementations from the current Energy Filtered Transmission Electron Microscopy examination. The round or diamond tips of the liberated goethite crystals suggest slow crystal growth in high silicate conditions. The effect of pre-treating the cementation structure by potassium hydroxide liquor digestion upon the atmospheric pressure acid leaching performance is also studied in this paper. Both particle size analysis using laser diffraction and direct imaging using Transmission Electron Microscopy confirm the effective disintegration of the cementations and the liberation of goethite crystals. As a result, the leaching rates of these nickel laterite ores increase by more than 6 times; nickel recoveries of these laterite ores are also increased from under 50% to near 90% after 16 h acid leaching. The accelerating effect of the potassium hydroxide pre-treatment upon acid leaching rates verified that an envelope of silica and/or silicates hindered the contact between acid and goethite crystals during atmospheric leaching of these nickel laterite ores.

1. Introduction

Some limonitic nickel laterite ores from Western Australia demonstrate radically different atmospheric pressure acid leaching (AL) performance even though these have similar mineralogical compositions (Watling et al., 2011). Such ores generally contain goethite, quartz, kaolinite, and minor amounts of iron oxides, spinels, and clay minerals (Landers et al., 2009a, 2009b; Watling et al., 2011). However, the way these mineral phases are assembled in Western Australian laterite ores was not studied. A previous investigation (Part I) of the micro-morphological characters of selected limonitic ores revealed a distinctive goethite morphology that differed from the conventional acicular shape (Wang et al., 2013). The ubiquitous sub-micrometer electron-optical dense particles in these ore samples were identified as goethite-silica/silicate cementations (terminology following Schwertmann, 1988; Schwertmann and Taylor, 1989), which are believed to be responsible for their slow acid leaching. These goethite-silica/silicate cementations are similar to those found in other states in Australia by Fordham and Norrish (1979, 1983), who used the terms "goethite pellet" and "microaggregates" to describe this form of goethite occurrence. The intimacy of iron oxide and clay particles has also been observed in silica-cementing goethite in fragipan soil samples from Northwestern Italy (Marsan and Torrent, 1989) and laterite ores in India (Das et al., 2010).

The paragenetic growth of goethite and kaolinite was found in samples from Cameroon (Boudeulle and Muller, 1988).

The previous study (Part I) (Wang et al., 2013) showed that caustic digestion is able to disassemble the cementation frameworks of acid resistant nickel laterite ores from Western Australia. Caustic digestion has long been used in Bayer process for aluminium extraction from bauxite (Smith, 2009) but has not been previously used as a nickel laterite pre-treatment to disintegrate its cementation structure. The effectiveness of using potassium hydroxide as a pre-treatment to facilitate the atmospheric acid leaching of these laterite ores is studied in this paper. Potassium hydroxide (KOH) rather than sodium hydroxide (NaOH) was used to avoid sodalite formation and improve silica removal from the solids (Lowe, 2007). KOH digestion was chosen to disintegrate goethite-silica/silicate cementations based on the following reactions:

$$SiO_2 + 2OH^- = SiO_3^{2-} + H_2O$$

$$Al_2Si_2O_5(OH)_4 + 6OH^- = 2SiO_3^{2-} + 2AlO_2^- + 5H_2O.$$
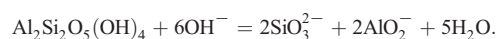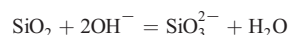
In order to better understand the mechanism of cementation breakage, the cementation structure before and after caustic digestion was further studied using Energy Filtered Transmission Electron Microscope (EFTEM). The EFTEM technique, which collects specified elemental information to form each image frame using a CCD camera, has a higher spatial resolution and faster response than STEM/EDS mapping. The

* Corresponding author.
  E-mail address: tony.wang@curtin.edu.au (X. Wang).

latter collects the whole EDS spot by spot and the spatial resolution is usually restricted by the spot size of the electron beam (Hofer and Warbichler, 2005). EFTEM maps of iron, silicon, aluminium, and oxygen are presented in this paper to provide direct evidence for the microstructure of goethite-silica/silicate cementations in nickel laterite ore samples from Western Australia.

2. Materials and methods

Based on the atmospheric pressure leaching data reported in Part I (Wang et al., 2013), two slow leaching limonitic nickel laterite ore samples, A15 and B11, were chosen to test the effect of liberating cementations on their AL performance. These ore samples were originally collected from mine sites within the Yilgarn Craton greenstone belt in Western Australia. The samples were screened to less than 2 cm and were sub-sampled using a riffle splitter to give 50 g fractions followed by a size reduction using a Rocklabs® model 1A ring mill to ensure all the powders have passed through a 70-mesh sieve (<212 μm).

In order to compare the leaching performance of the laterite ores A15 and B11 before and after KOH treatment, the two selected powder samples A15 and B11 were first digested using KOH liquor in an autoclave and then leached by sulphuric acid using the same AL conditions used in Part I (Wang et al., 2013).

2.1. Potassium hydroxide treatment

In order to deliberately break up the goethite-silica/silicate cementations, the slow leaching laterite ore powder samples A15 (89.3 g) and B11 (90.1 g) were digested with 9 L of 5 M potassium hydroxide (reagent grade KOH, Sigma-Aldrich) liquor in a Parr 5 gal. 316 stainless steel autoclave in atmospheric pressure at 95 °C with 450 rpm agitation rate using a dual pitch blade impeller for 5.5 h. Pulps were taken from the autoclave at the end of the digestion and filtered. The collected solids were redispersed in deionised water and washed several times before drying overnight at 70 °C. The pregnant liquor and the dried solids were analysed by ICP-OES. The phase compositions of the residual solids were determined by quantitative phase analysis (QPA) using laboratory-based X-ray diffraction (XRD). The particle morphologies of the KOH-treated residues were imaged by TEM.

2.2. Sulphuric acid leaching

The KOH-treated residues of samples B11 (62.3 g) and A15 (77.2 g) were then leached separately using sulphuric acid in atmospheric pressure at 95 °C in a Parr 1 gal. titanium autoclave for 16 h. Slurries consisting of approximately 9 wt.% solids and 2000 kg/t sulphuric acid with total volume of 600–700 mL were employed. A dual pitch blade impeller was employed to provide a 500-rpm agitation rate. Pulps were taken from the autoclave at selected reaction times, and the primary filtrates were collected through a 0.45-μm Supor® membrane. The solids were repulped and washed with deionised water several times then dried overnight at 70 °C. The primary filtrate and dried solids were analysed by ICP-OES to determine metal concentrations and

estimate the leaching rates. As there was some sample bias toward liquor content in samples, the "Solver" tool in Microsoft® Excel was used to refine the solid to liquid ratio in the autoclave to optimise mass balances based on the ICP-OES assays for both filtrate and solids. The solids weight losses during acid leaching were calculated from the refined solid to liquid ratio. The solids were also examined by laboratory-based XRD for QPA.

2.3. Particle size analysis

The particles sizes of sample A15 and B11 were measured using a Malvern® laser diffraction particle size analyser (Mastersizer 2000) after dispersing the powders in deionised water in an ultrasonic bath for 5 min.

2.4. Inductively coupled plasma emission spectrometry

The metal concentrations and chemical compositions of all samples were determined by inductively coupled plasma emission spectrometry (ICP-OES). The solid samples were analyzed after fusion with Sigma Chemicals 12:22 lithium borate flux and subsequent dissolution in water.

2.5. X-ray diffraction

The particle size of the solid samples was further reduced using a McCrone® micronising mill for 5 min. Laboratory grade ethanol (5 mL/g) was chosen to assist milling and corundum pellets were used as the milling medium. Approximately 10 wt.% of corundum (Alumina polishing compound, Praxair Surface Technologies, Inc.) was added as an internal standard prior to micronising, and the milled slurries were dried at 70 °C before packing into 25 mm diameter flat plate plastic holders. Corundum was chosen because it has a mass absorption coefficient similar to quartz, goethite, and nontronite for CoK_α radiation, reducing micro-absorption effects in the quantitative analyses (Madsen and Scarlett, 2008).

The XRD patterns of the samples were obtained using a Bruker® D8 Discover diffractometer using Bragg-Brentano geometry on a 217.5-mm goniometer with CoK_α radiation. The data were collected by Bruker® LynxEye PSD from 5° to 90° 2θ with a step size of 0.01° 2θ at 0.5 s per step, using a 0.3° fixed divergence slit and 2.5° primary and secondary Soller slits. These instrument settings were used in the fundamental parameters approach to determine instrumental contributions to peak profiles (Cheary and Coelho, 1992).

2.6. Transmission electron microscopy and energy-dispersive spectroscopy

Powder samples were dispersed in deionised water and agitated in an ultrasonic bath for 5 min. A drop of the suspension for each sample was air dried on carbon film supported by a 3-mm diameter copper grid. A JEOL® 2011 transmission electron microscope (TEM) operated at 200 kV and equipped with a Gatan® digital camera was used to image the particle morphologies and an Oxford Instruments INCA® 200 EDS

Table 1
Quantitative phase analysis results for samples A15 and B11 before and after KOH treatment based on the XRD patterns. The figures in brackets represent Rietveld calculation errors in the last decimal places.

Sample (wt.%)	Goethite	Quartz	Hematite	Maghemite	Kaolinite	Nontronite	Amorphous
A15 feed ore	49.07(23)	25.17(14)	–	0.845(95)	3.77(32)	–	21.1(10)
A15 digested	57.73(19)	29.09(13)	–	1.22(16)	–	–	12.0(13)
B11 feed ore	41.93(67)	5.89(11)	1.52(19)	8.44(19)	9.92(43)	4.88(33)	27.4(12)
B11 digested	56.75(21)	7.016(70)	1.92(18)	11.17(14)	–	–	23.1(11)